Electronic Supplementary Material (ESI) for Materials Advances.

Supporting Information

One-Pot Route to Fine-Tuned Hypercrosslinked Polymer Solid Acid Catalysts

Alexander Blocher,[a+] Florian Mayer,[a+] Paul Schweng,[a] Teresa M. Tikovits,[a] Neptun Yousefi,[a] Robert T. Woodward[a*]

[a]Institute of Materials Chemistry and Research, Faculty of Chemistry, University of Vienna, Währinger Straße 42, 1090 Vienna, Austria

[+]These authors contributed equally to this work.
*email: robert.woodward@univie.ac.at

1. Experimental

1.1. Materials

1,2-Dichloroethane (≥99.0%, ACS reagent), 4,4‘-bis(chloromethyl)-1,1‘-biphenyl (95%), Chlorosulfonic acid (99%), and cyclohexyl acetate were purchased from Sigma-Aldrich. Methanol (≥99.8%) was purchased from Fisher Scientific.

1.2. Synthesis of sulfonated hypercrosslinked polymers

4,4‘-Bis(chloromethyl)-1,1‘-biphenyl (2 mmol, 0.502 g) was first dissolved in 1,2-dichloroethane (DCE, 5 mL) at room temperature and stirred for 10 min at ~150 rpm. Subsequently, the solution was cooled to ~0 °C using an ice bath and stirred again for a period of 10 min. Afterwards, the speed was switched to ~250 rpm and a solution of chlorosulfonic acid (8, 6, 5, 4, 3, 2, 1.5, 1, 0.5 or 0.25 mmol) in DCE (1 mL) was added. After 15 min a reflux condenser was attached to the reaction and the ice bath was replaced with an oil bath. The solution was then heated to 80 °C for 22 h. After heating, the resulting brown/black solid was washed with 50 mL of methanol in a Buchner funnel before being washed overnight via Soxhlet extraction, again with methanol. In order to remove excess methanol from the washing procedure, the polymer was allowed to dry for a few hours at room temperature. Finally, it was dried in a vacuum oven at 60 °C overnight.

1.3. Hydrolysis of cyclohexyl acetate using sulfonated hypercrosslinked polymers

Cyclohexyl acetate (1 g), distilled water (4 g) and acid catalyst (0.1 g) were added into a pressure-resistant reaction tube (15 mL) equipped with a magnetic stir bar. The reaction tube was then placed in a preheated oil bath at 120 °C and stirred at 800 rpm for 3 h. Afterwards, the reaction solution was washed twice with 10 mL ethyl acetate, filtered using syringe filters and dried over $MgSO_4$. The resulting organic phase was analysed using GC-MS after further dilution in ethyl acetate.

1.3. Characterisation

Fourier-transform infrared spectroscopy was performed on finely ground samples in the range 350-4000 cm^{-1} using a Tensor II FT-IR Spectrometer from Bruker.

Solid-state NMR was carried out on a Bruker Avance NEO 500 wide bore system (Bruker BioSpin, Rheinstetten, Germany) using a 4 mm triple resonance magic angle spinning probe. Between 15 - 25 mg of material was packed into a 4 mm zirconia CRAMPS rotor. The resonance frequency for ^{13}C NMR was 125.78 MHz, the MAS rotor spinning was set to 14 kHz. Cross polarisation was achieved by a ramped contact pulse with a contact time of 3 ms. During acquisition ^1H was high power decoupled using SPINAL with 64 phase permutations. The ^1H $\pi/2$ pulse was 2.5 μs, the relaxation delay was set to 4 s, and with roughly 2000 scans a sufficient signal to noise was achieved. The chemical shifts for ^{13}C are reported in ppm and are referenced external to adamantane by setting the low field signal to 38.48 ppm.

Powder X-ray diffraction (PXRD) measurements were performed on a Malvern Panalytical Empyrean instrument in reflectance mode configuration using Cu $K\alpha_{1+2}$ radiation (wavelength of 1.5406 Å). Measurements were taken using a step size of 0.0263 °2θ, generator settings of 40 mA and 45 kV at a measurement temperature of 25 °C. The scan range is 5 to 50° with a scan step time of 59.4 s.

Elemental analysis was performed using a Eurovector EA 3000 CHNS-O Elemental Analyser. Between 0.75 and 3.0 mg of each sample was weighed into tin vials (4×6 mm) for each individual run and each sample was ran at least in duplicate. Sample weighing is done using a micro balance (Sartorius, ME 5 OCE) for accuracy. The operating temperatures for the combustion and reduction were 1000 °C (1480 °C for O analysis) and 750 °C, respectively, with high purity helium (99.999+) used as a carrier gas.

X-ray photoelectron spectroscopy (XPS) was performed on a Nexsa Photoelectron Spectrometer (Thermo Scientific, UK). For each sample a survey spectrum was collected with a step size of 1 eV and a pass energy of 200 eV. Furthermore, element specific high-resolution spectra for Carbon (C1s 279-298 eV) Nitrogen (N1s 392-410 eV), Oxygen (O1s 525-545 eV), Chlorine (Cl2p 190-210 eV) and Sulphur (S2p 157-175 eV) with step sizes of 0.1 eV and a pass energy of 50 eV were acquired. All measurements were performed using Al-Kα X-rays with a spot size of 400 µm. A second set of XPS measurement was performed on a set of samples after BET analysis to gain information if changes in the chemical bonding structure occurs when drying at 120 °C.

Dynamic Vapour Sorption (DVS) experiments were performed using a DVS-Resolution (Surface Measurement Systems, UK). For each run, approximately 10 mg of sample was weighed into a quartz crystal pan. Deionised water was used to generate the desired relative humidity (RH) for the three-step measurement program. In the first step, the sample was dried for 24 h at 0 % RH before the RH was increased to 90 % for 24 hours for water uptake. A final desorption step followed at 0 % RH for 24 h. The experiments were carried out at 25 °C.

To determine the porous properties of SHCPs, nitrogen adsorption-desorption isotherms were measured at -196 °C using a TriStar II from Micromeritics Instrument Corporation, controlled by the software TriStar II 3020 version 3.02. Samples were degassed for at least 4 h at 120 °C under N_2 using a FlowPrep 060 from Micromeritics Instrument Corporation. Data evaluation was performed using VersaWin^{TM} software version 1.0. Sample surface areas were calculated using the Brunauer-Emmett-Teller (BET) method on the adsorption branch between 0.05 - 0.2 P/P_0. The total pore volume, V_{TOT}, was calculated from the volume of N_2 adsorbed at $P/P_0 = 0.97$. The micropore volume, V_{MICRO}, was determined using the t-plot method for the relative pressure range between 0.15 – 0.4.

Thermal analyses were performed using a Discovery TGA from TA instrument. Approximately 20 mg of each sample was heated from room temperature both under either air or N_2 gas flow (100 $mL \cdot min^{-1}$) to 110 °C at a rate of 10 $°C \cdot min^{-1}$ and held at this temperature for 15 min. Following the isothermal step, samples were heated to 800 °C at a rate of 10 $°C \cdot min^{-1.}$

Transmission electron microscope images were captured using a Philips CM200 TEM equipped with a camera (Orius SC600 CCD) and was used at 200 kV to observe the polymers. To prepare the samples for imaging, dilute ethanol suspensions of the networks were prepared (3 g/L). The TEM grips were dipped into the suspensions and allowed to dry before the measurement.

To determine the conversion of cyclohexyl acetate to cyclohexanol, a coupled gas chromatography (Agilent Technologies 7890A with column Agilent 19091S-433UI) – mass spectrometry (Agilent Technologies 5975C) setup with attached Injector (Agilent Technologies 7683B Series) was used. Injecting sample volume was 1 µL with He as carrier gas and the temperature program as follows: equilibrate at 35 °C with isotherm for one min, ramp at 20 °C/min until 300 °C, isotherm for 3.5 min. Prior to measurement all samples were diluted 1:50 with ethyl acetate resulting in a total sample dilution of 1:10,000. The corresponding chromatogram was evaluated with a provided program (Masshunter) as well as manually with a prior extraction of the data from the GC-MS system. Finally, the conversion of cyclohexyl acetate was determined by comparing the integrated peak areas of compounds present.

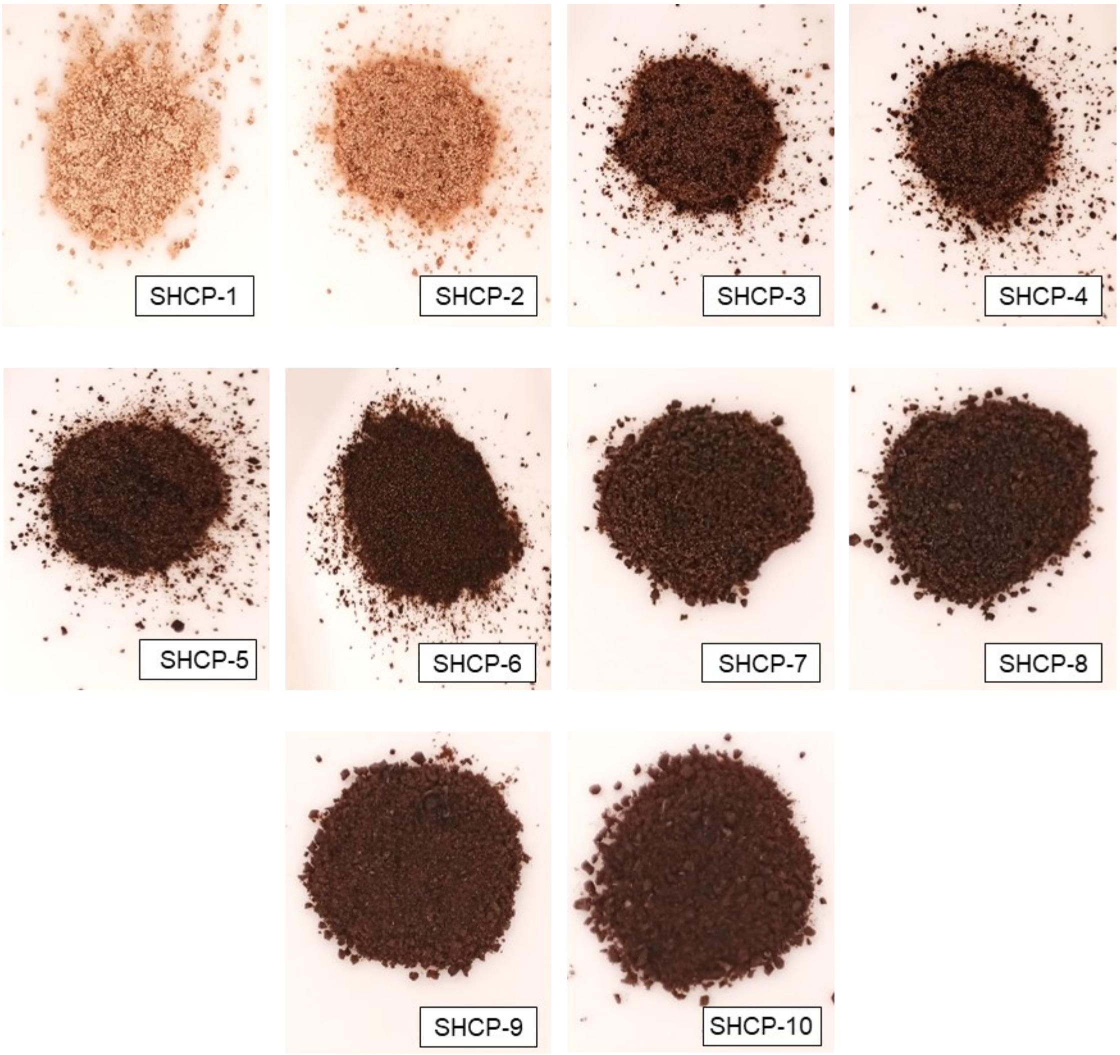

Figure S1. Photographs of all SHCPs.

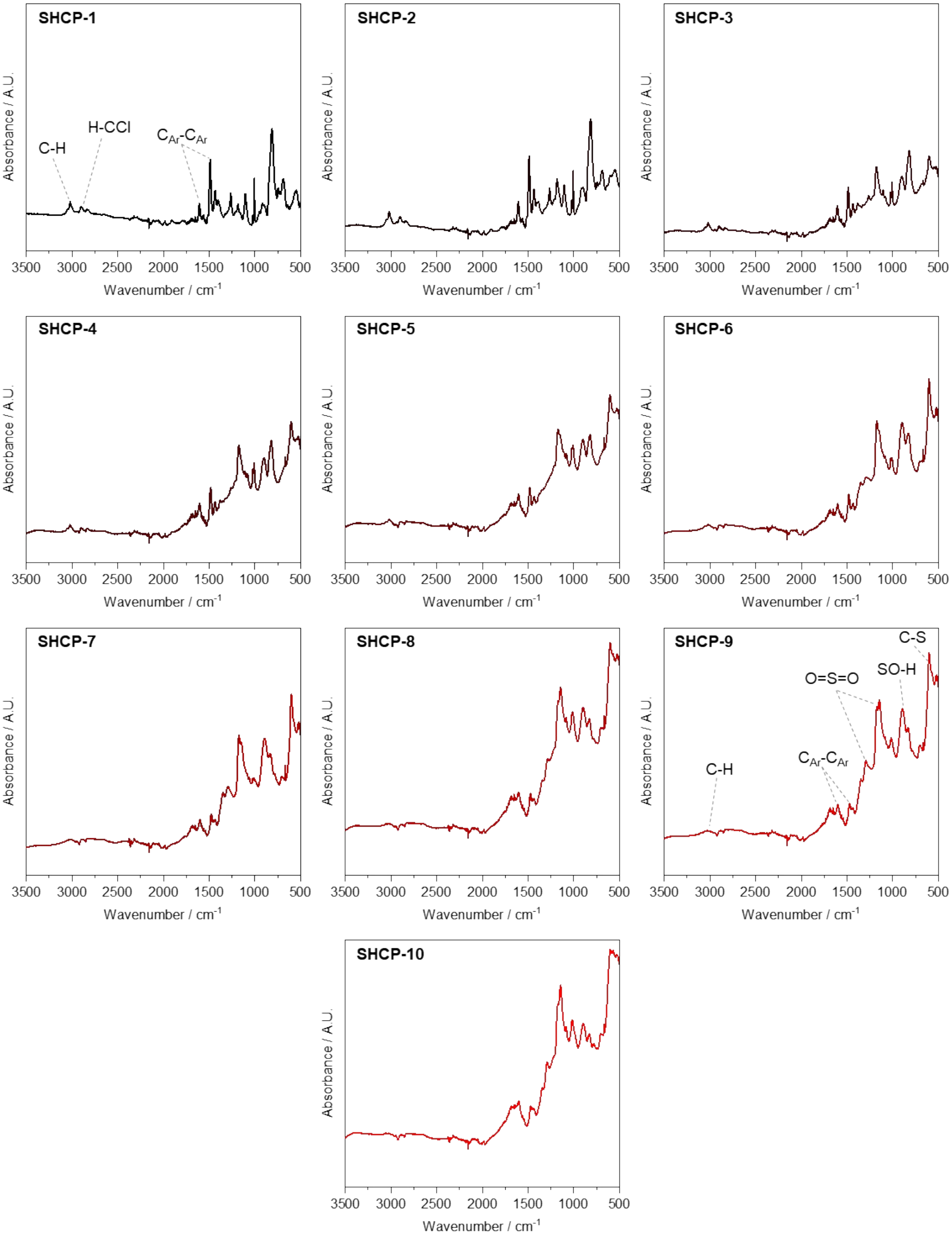

Figure S2. FTIR spectra of all SHCPs. Measured upon removal from a drying oven, where they were stored at 60 °C.

Table S1. Elemental composition of SHCP-1 to SHCP-10 derived from XPS analysis. Sulfur content is included in both at.% and mmol·g^{-1}. The numbers provided here represent an average and standard deviation across three synthesis repeats, unless stated otherwise.

	C (at.%)	Cl (at.%)	S (at.%)	S (mmol·g^{-1})	O (at.%)
SHCP-1	97.5 ± 0.6	1.4 ± 0.2	0.1 ± 0.0	0.1 ± 0.0	1.0 ± 0.1
SHCP-2	96.3 ± 0.8	0.8 ± 0.1	0.5 ± 0.1	0.4 ± 0.1	2.5 ± 0.2
SHCP-3	92.5 ± 1.0	0.5 ± 0.0	1.7 ± 0.0	1.3 ± 0.0	5.6 ± 0.0
SHCP-4	89.6 ± 1.8	0.5 ± 0.1	2.6 ± 0.2	2.0 ± 0.1	8.0 ± 0.5
SHCP-5	85.8 ± 0.9	0.5*	3.5 ± 0.1	2.6 ± 0.1	10.5 ± 0.5
SHCP-6	82.5 ± 1.6	0.5 ± 0.0	4.4 ± 0.2	3.3 ± 0.1	13.3 ± 0.3
SHCP-7	78.4 ± 1.4	0.5 ± 0.0	5.7 ± 0.3	4.1 ± 0.2	16.0 ± 0.3
SHCP-8	77.0 ± 2.2	0.7 ± 0.1	6.1 ± 0.0	4.3 ± 0.0	17.2 ± 0.2
SHCP-9	76.2*	0.6*	6.5*	4.6*	18.3*
SHCP-10	74.4 ± 2.2	0.8*	6.6 ± 0.1	4.6 ± 0.1	19.0 ± 0.2
SHCP-6[a]	80.8	-	4.7	3.4	13.5
SHCP-7[a]	78	-	5.8	4.2	15.4

*Obtained from an average of two samples due to peak shifting preventing the third analysis.
[a]After heating to 120 °C to investigate -SO_3H stability

Table S2. Elemental composition of SHCP-1 to SHCP-10 derived from CHNS-O elemental analysis. Sulfur content is included in both wt.% and mmol·g^{-1} for ease of comparison. The numbers provided here represent an average and standard deviation across three synthesis repeats.

	C (wt.%)	H (wt.%)	O (wt.%)	S (wt.%)	S (mmol·g^{-1})
SHCP-1	87.42 ± 4.24	5.65 ± 0.35	1.20 ± 0.39	0.11 ± 0.06	0.03 ± 0.02
SHCP-2	84.11 ± 3.80	5.46 ± 0.27	4.69 ± 0.24	1.39 ± 0.19	0.44 ± 0.06
SHCP-3	78.01 ± 0.70	5.34 ± 0.14	11.09 ± 1.35	3.69 ± 0.18	1.15 ± 0.06
SHCP-4	71.98 ± 3.56	5.15 ± 0.15	15.16 ± 1.83	5.51 ± 0.27	1.72 ± 0.08
SHCP-5	67.15 ± 2.95	5.08 ± 0.32	20.34 ± 1.99	7.03 ± 0.40	2.20 ± 0.13
SHCP-6	64.69 ± 2.11	4.83 ± 0.16	21.54 ± 2.74	9.03 ± 0.29	2.82 ± 0.09
SHCP-7	58.48 ± 3.23	4.77 ± 0.37	29.91 ± 2.59	10.38 ± 0.51	3.24 ± 0.16
SHCP-8	56.81 ± 2.87	4.70 ± 0.33	28.45 ± 5.55	10.87 ± 0.37	3.40 ± 0.12
SHCP-9	55.49 ± 3.46	4.49 ± 0.38	29.40 ± 5.49	11.53 ± 0.56	3.60 ± 0.17
SHCP-10	54.57 ± 2.86	4.44 ± 0.33	32.83 ± 1.58	12.02 ± 0.36	3.76 ± 0.11

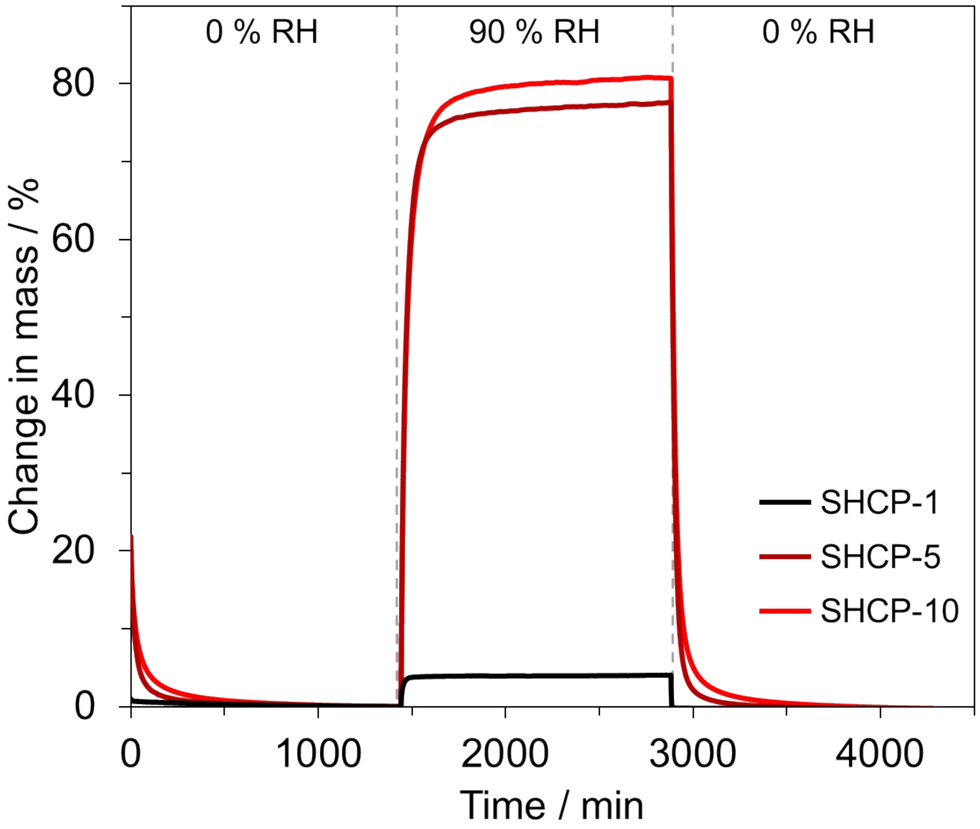

Figure S3. Water vapour sorption of SHCP-1 (black), SHCP-5 (maroon) and SHCP-10 (red) determined by dynamic vapour sorption. Grey dotted lines indicate a change in relative humidity (RH). All measurements were performed at 25 °C.

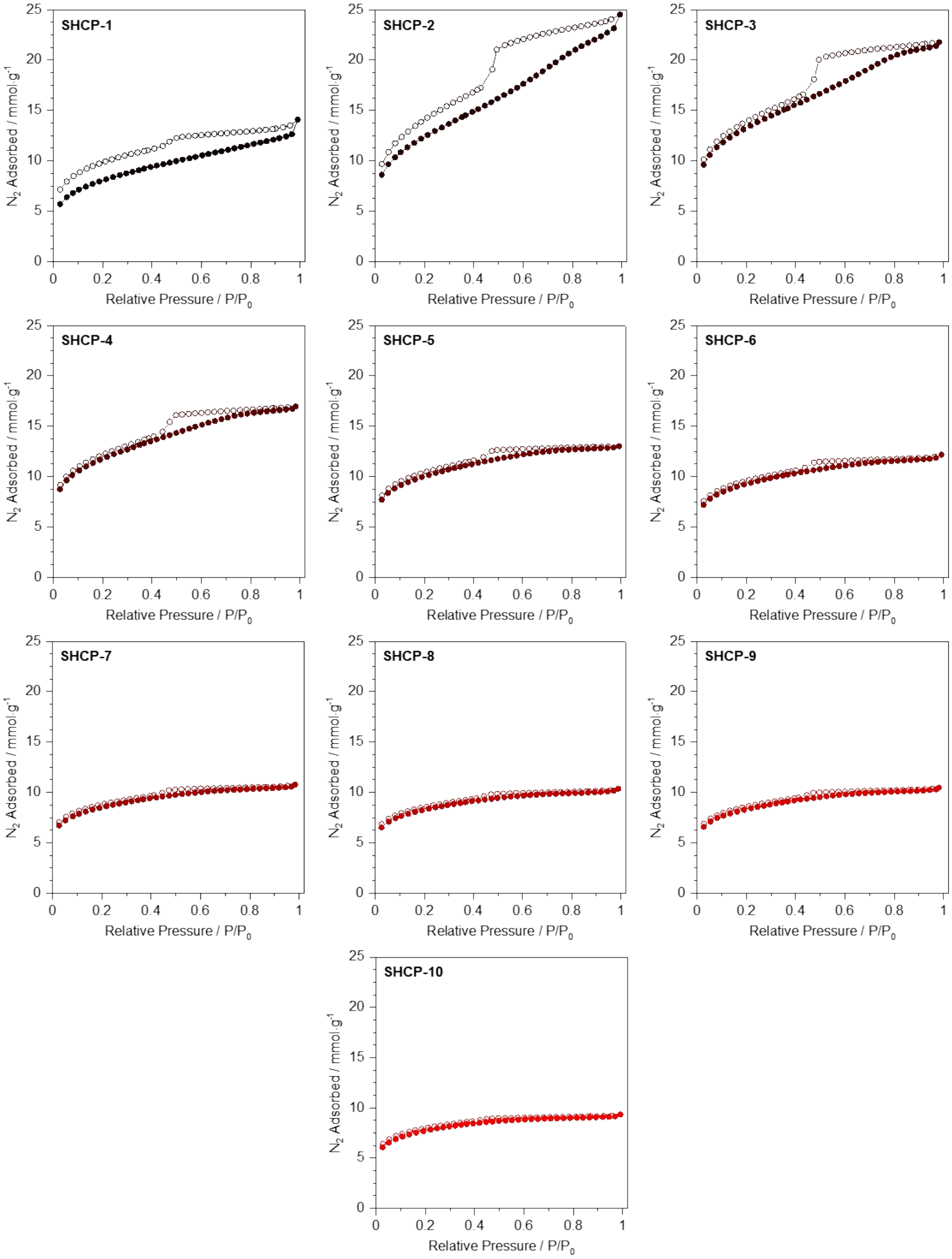

Figure S4. A representative set of N_2 sorption isotherms of all SHCPs measured at 77 K.

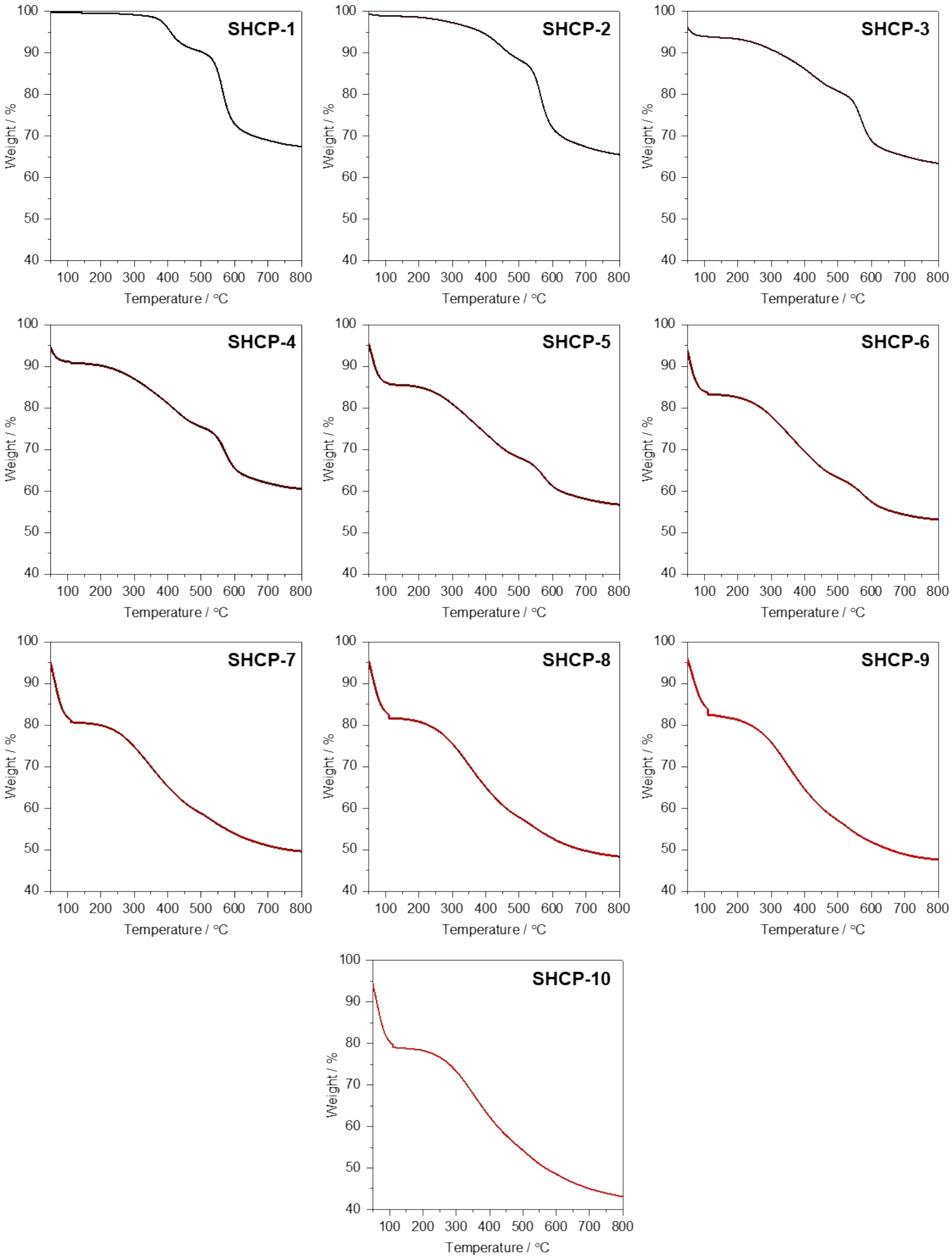

Figure S5. Thermogravimetric curves for all SHCPs under N_2 flow (100 mL·min^{-1}), ramped to 800 °C at a rate of 10 °C/min. A 10 min isothermal step was included at 110 °C.

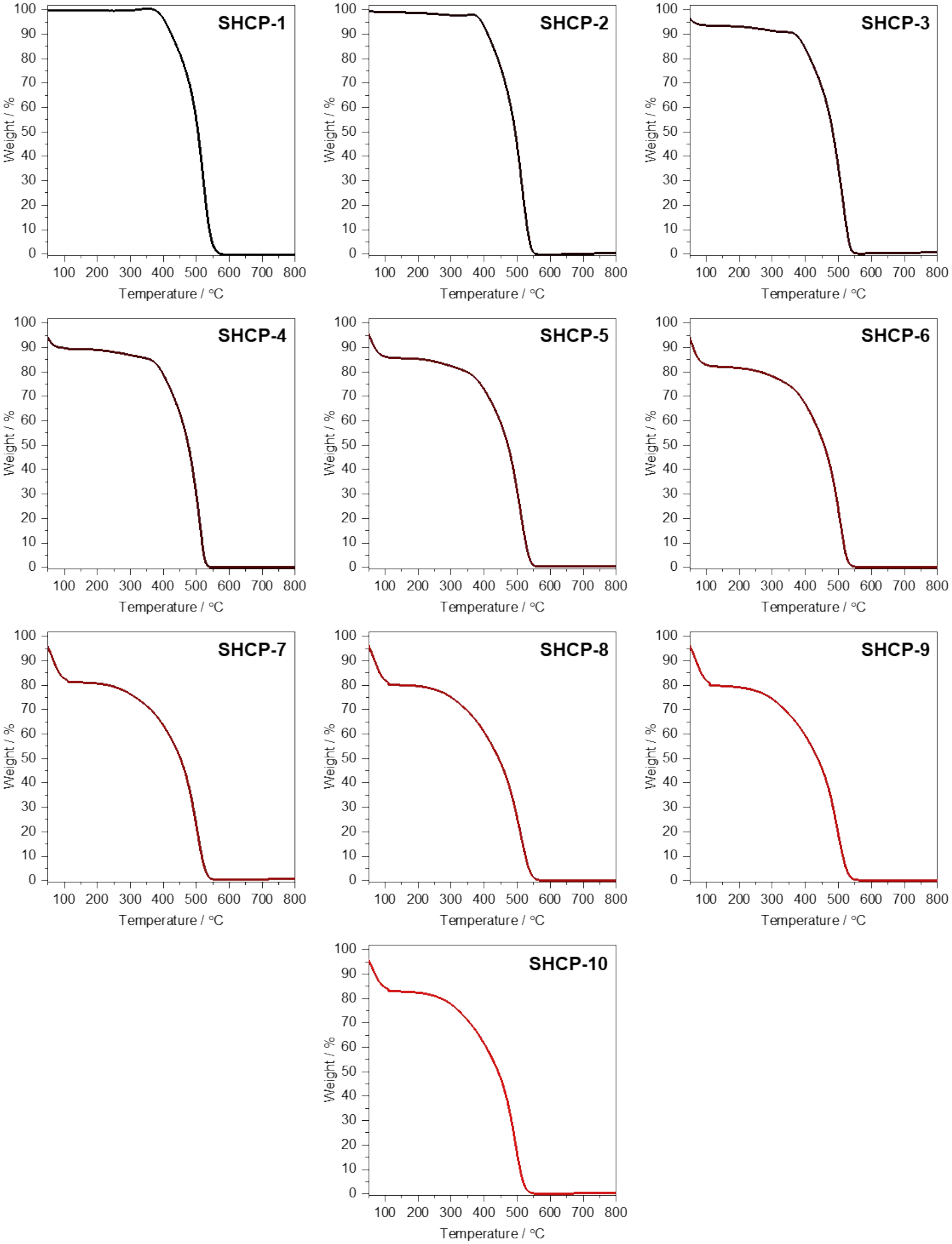

Figure S6. Thermogravimetric curves for all SHCPs under air flow (100 mL·min^{-1}), ramped to 800 °C at a rate of 10 °C/min. A 10 min isothermal step was included at 110 °C.

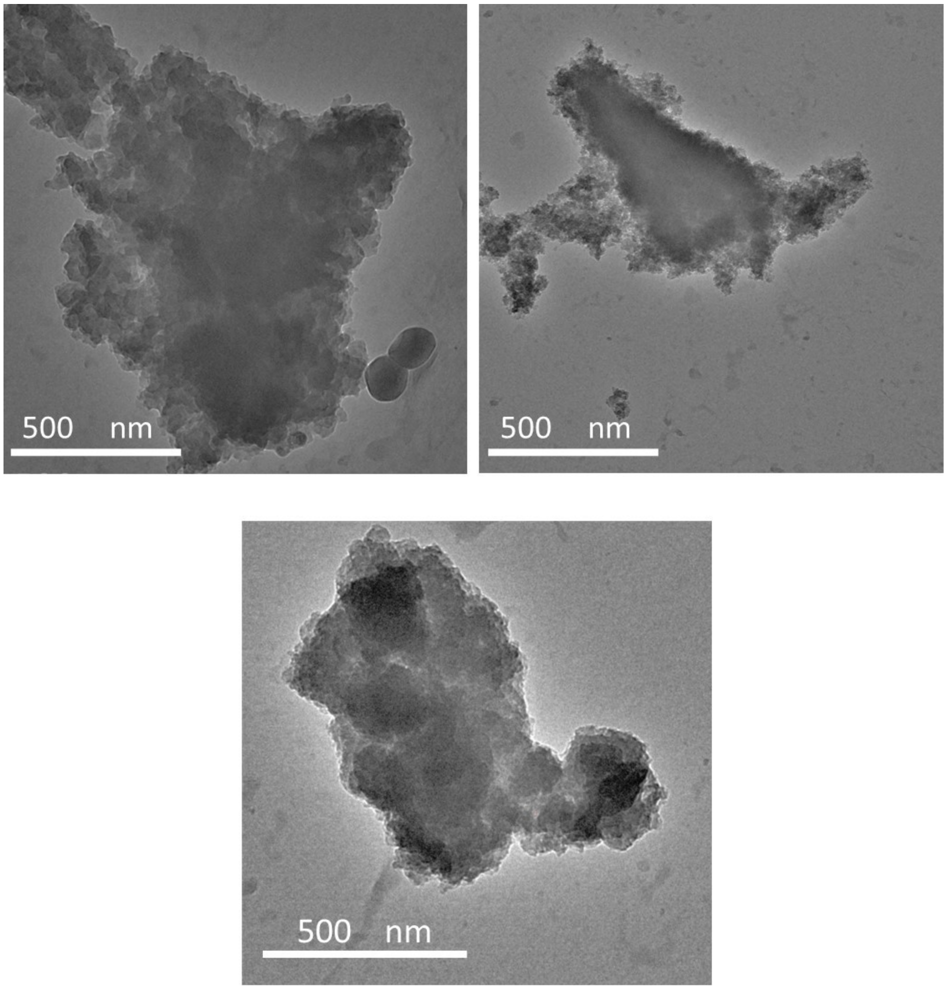

Figure S7. TEM images of SHCP-10 (left, top), SHCP-5 (right, top) and SHCP-1 (bottom).

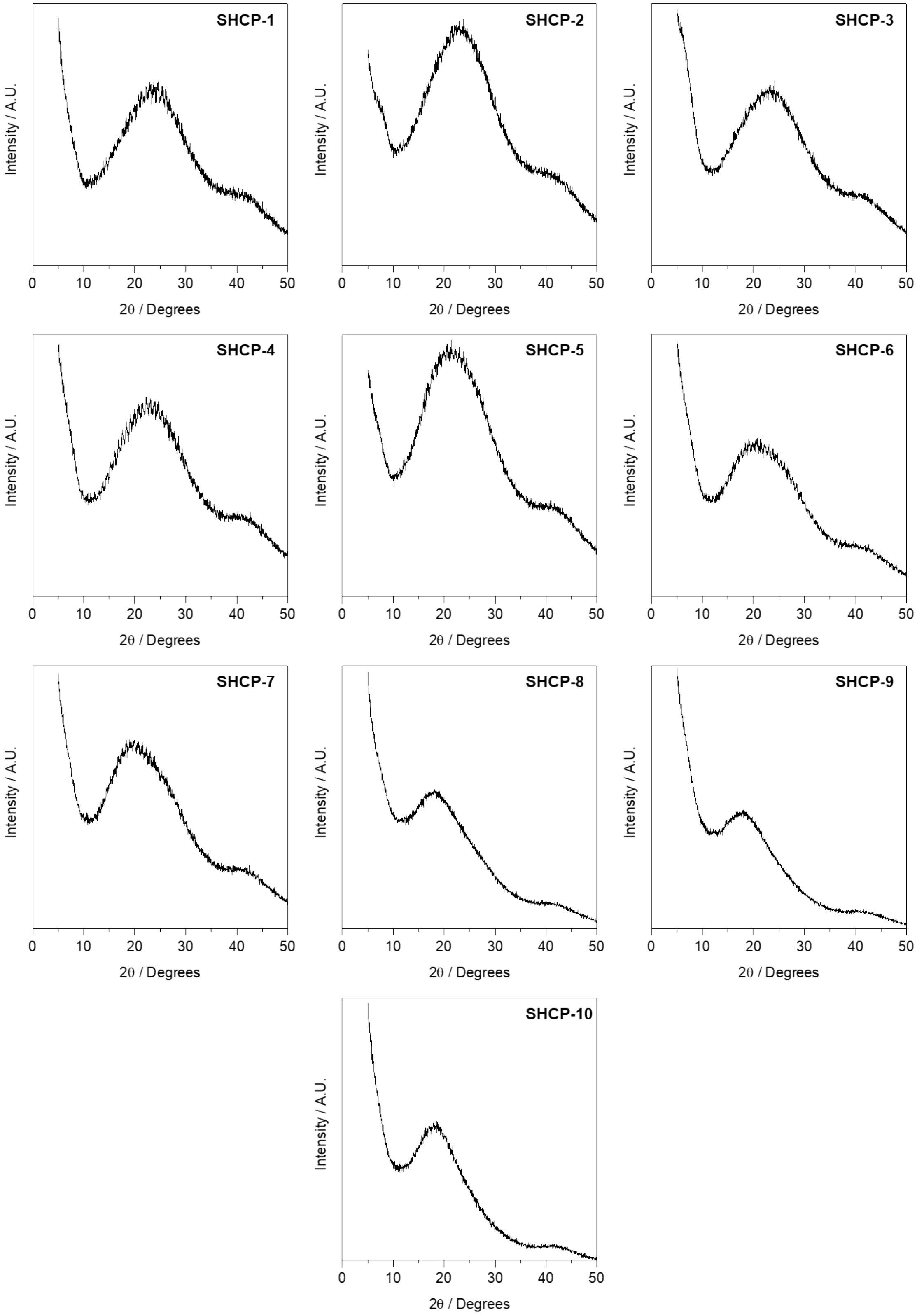

Figure S8. Powder X-ray diffraction patterns of sulfonated hypercrosslinked polymers SHCP-1 – SHCP-10.

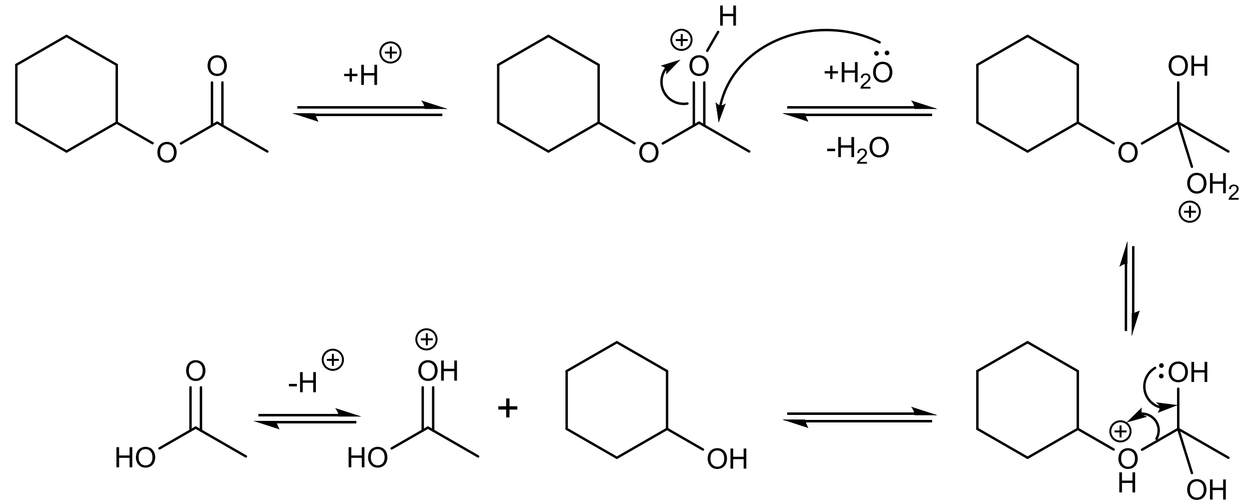

Figure S9. Reaction mechanism of cyclohexyl acetate hydrolysis to cyclohexanol and acetic acid.

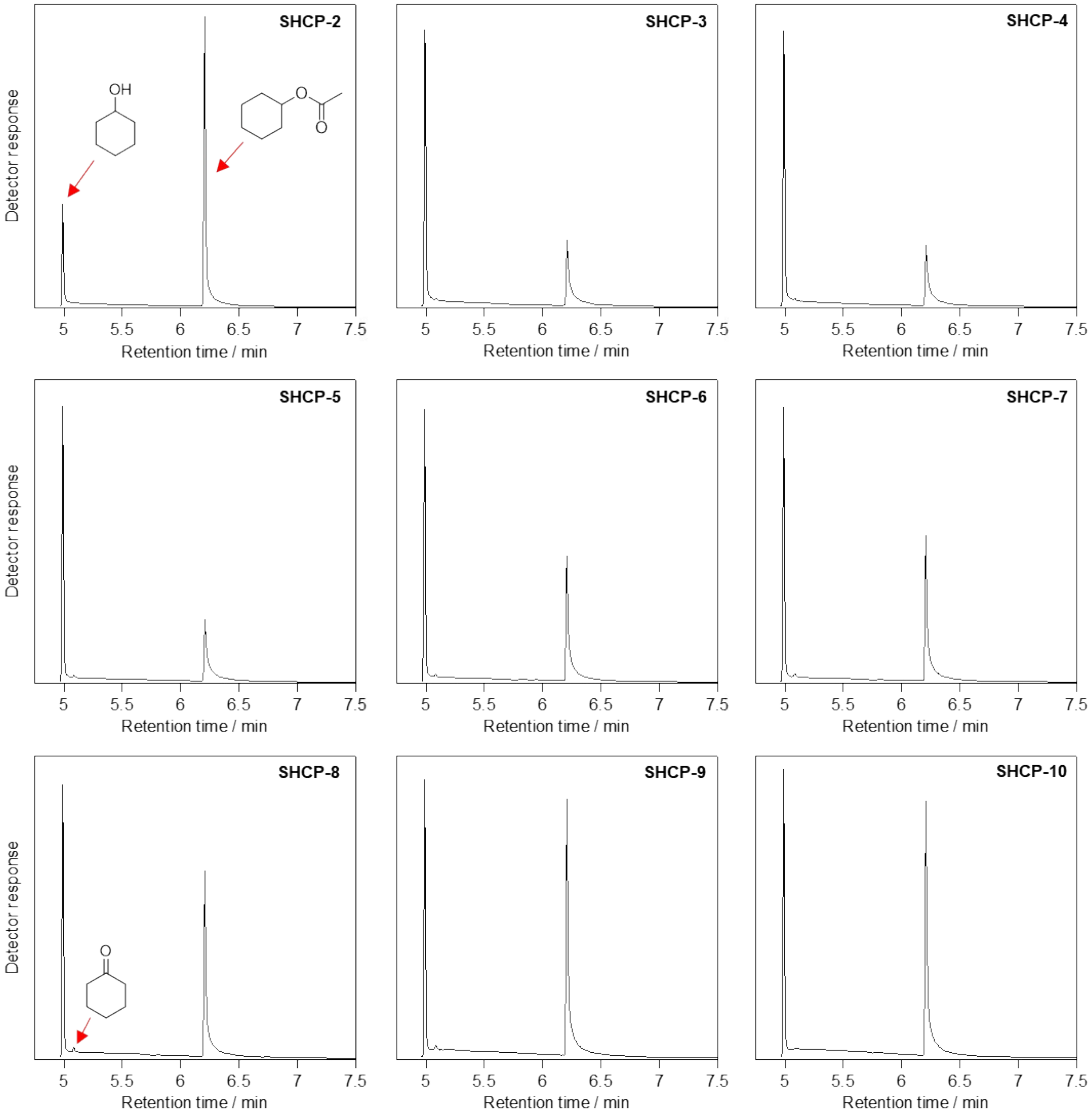

Figure S10. Typical GC traces of catalysis products for SHCP-2 – SHCP-10. SHCP-1 is excluded as it showed no product formation.

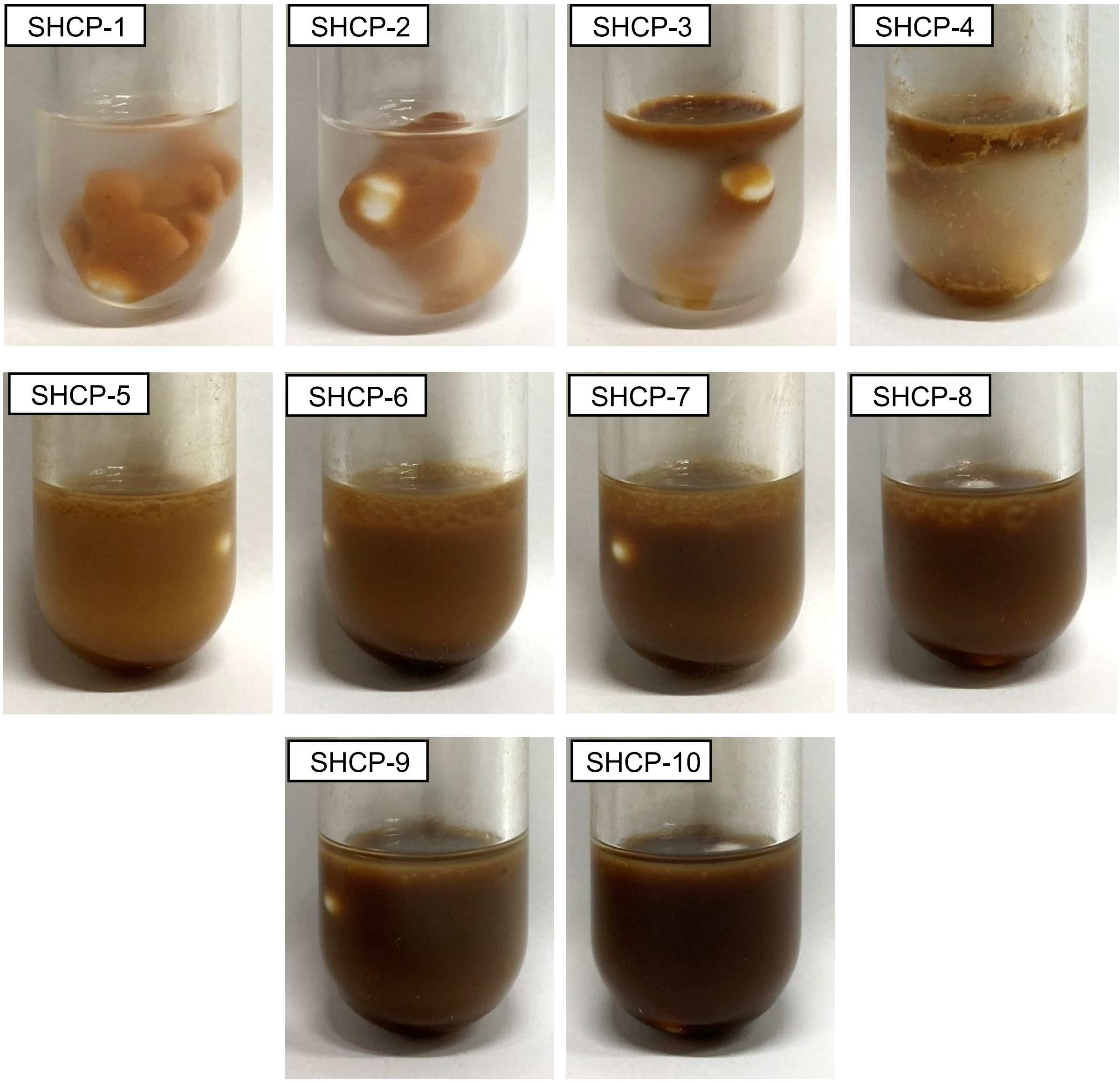

Figure S11. Photographs of all polymers in cyclohexyl acetate/cyclohexanol-water two phase systems, post-catalysis reaction.

Table S3. Elemental composition of SHCP-5 before and after use as a solid acid catalyst derived from CHNS-O elemental analysis. Sulfur content is included in both wt.% and mmol·g^{-1} for ease of comparison.

	C (wt.%)	H (wt.%)	O (wt.%)	S (wt.%)	S (mmol·g^{-1})
SHCP-5	67.2 ± 3	5.1 ± 0.3	20.3 ± 2.0	7.0 ± 0.4	2.2 ± 0.1
SHCP-5 post-conversion	59.4 ± 0.2	4.9 ± 0.2	24.2 ± 1.2	7.0 ± 0.02	2.18

Table S4. Elemental composition of SHCP-5 before and after use as a solid acid catalyst derived from XPS. Sulfur content is included in both wt.% and mmol·g^{-1} for ease of comparison.

	C (at.%)	Cl (at.%)	O (at.%)	S (at.%)	S (mmol·g^{-1})
SHCP-5 (XPS)	85.8 ± 0.9	0.5*	10.5 ± 0.5	3.5 ± 0.1	2.6 ± 0.1
SHCP-5 post-conversion (XPS)	83.6	0.2	11.9	3.5	2.7

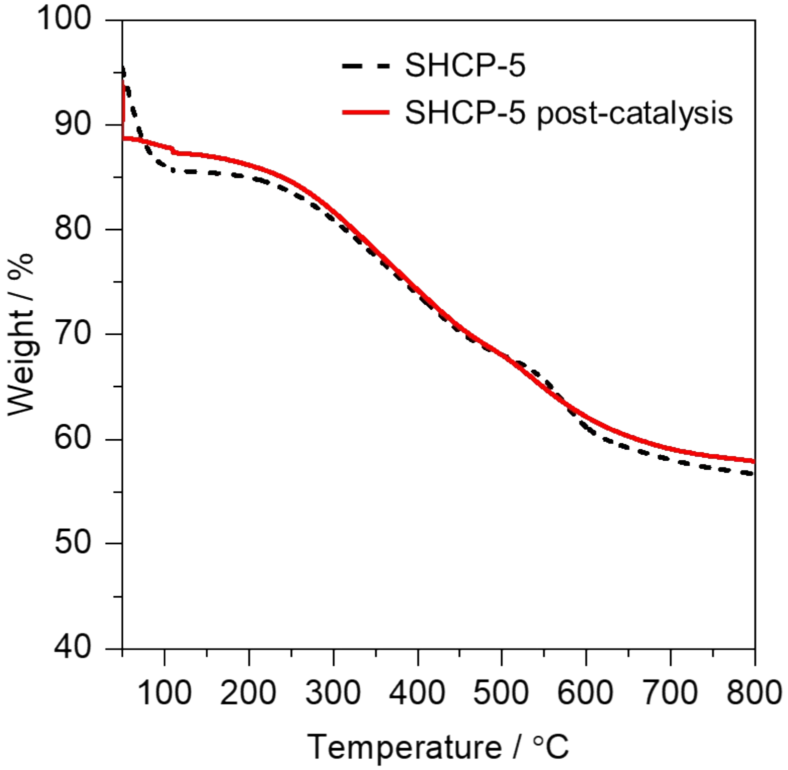

Figure S12. Thermogravimetric curves of SHCP-5 both before and after use as a solid acid catalyst. Analysis was performed under N_2 flow (100 mL·min^{-1}) and ramped to 800 °C at a rate of 10 °C/min. A 10 min isothermal step was included at 110 °C.